

The infrared spectrum of magnesium oxide: a diode laser study using the discharge-enhanced reaction between hot magnesium vapor and N₂O

Svatopluk Civiš¹, Hartmut G. Hedderich^{2,3} and Cornelis E. Blom⁴

Physikalisch-Chemisches Institut der Justus-Liebig-Universität, Heinrich-Buff-Ring 58, W-6300 Giessen, Germany

Received 24 September 1990; in final form 6 November 1990

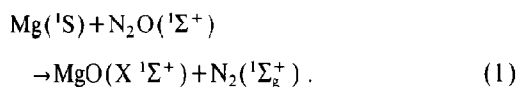
The high-resolution infrared spectrum of magnesium oxide is reported. The oxide was produced by a low-pressure discharge-enhanced reaction between hot magnesium vapor and nitrous oxide. Fifteen rovibrational transitions of the fundamental band and seven transitions of the first hot band of MgO(X¹Σ⁺) were detected with tunable diode lasers. The infrared transitions were combined with data from previous microwave and optical studies to yield precise spectroscopic constants for the X¹Σ⁺ and B¹Σ⁺ states of MgO.

1. Introduction

The rotational analysis by Lagerqvist [1] and Lagerqvist and Uhler [2] of the red and the green bands of magnesium oxide, first observed by Mahanti [3], has guided numerous studies on electronic bands of MgO. References to the earlier spectroscopic papers are given by Ikeda et al. [4]. Although the relative positions of the ground state (X¹Σ⁺) and the two low-lying electronic states a³Π (*T*_e=2619.86 cm⁻¹) and A¹Π (*T*_e=3563.3 cm⁻¹) are fixed [4,5], the strong mixing of these three states [6] certainly justifies further high-resolution spectroscopic studies. More recently, Azuma et al. [7] measured the 0-0 and 1-1 bands of the B¹Σ⁺-X¹Σ⁺ system with Doppler-limited resolution, whereas Törring and Hoefl [8] detected pure rotational transitions of

MgO(X¹Σ⁺). In the present study, we report the first observation of rovibrational transitions of MgO(X¹Σ⁺). In a merged fit to the optical [7], microwave [8], and the infrared data, a set of molecular constants for the X¹Σ⁺ and B¹Σ⁺ states has been obtained.

The alkaline earth-metals calcium, strontium and barium readily react with nitrous oxide in the gas phase. In contrast, the reaction between magnesium vapor and N₂O is strongly hindered under single-collision conditions. Experimental [9-11] and theoretical [12] studies have established the existence of an activation barrier for the reaction of ground-state magnesium with N₂O:



Breckenridge and Umernoto [9] showed that MgO can be formed by reaction (1), provided that the oven temperatures are sufficiently high. Subsequently, Törring and Hoefl [8] observed rotational transitions of MgO(X¹Σ⁺) in a low-pressure flame by passing N₂O through the Broida-type oven in which the magnesium was evaporated.

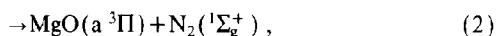
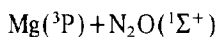
Following the theoretical study of Yarkony [12], the reaction of Mg(³P) and N₂O,

¹ Present address: J. Heyrovský Institute of Physical Chemistry and Electrochemistry, Czechoslovak Academy of Sciences, Dolejškova 3, 182 23 Prague 8, Czechoslovakia.

² Part of the author's dissertation, Justus-Liebig-Universität Giessen D 26, Germany.

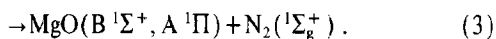
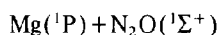
³ Present address: The University of Arizona, Department of Chemistry, Tucson, AZ 85721, USA.

⁴ Present address: Institut für Meteorologie und Klimaforschung, Kernforschungszentrum Karlsruhe, Postfach 3640, W-7500 Karlsruhe, Germany.

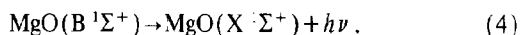


is largely downhill. However, at low pressure, the formation of $\text{MgO}(X\ ^1\Sigma^+)$ by reaction (2) is not likely, since triplet-singlet transitions are strongly forbidden. At higher pressures, ground-state MgO may be populated from the $a\ ^3\Pi$ state by inelastic collisions, but pressure broadening and cluster formation [13] put limits on the pressure-range available for high-resolution infrared spectroscopy.

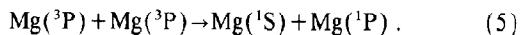
From a laser-induced-fluorescence study on the kinetics of the reaction between $\text{Mg}(^3\text{P}, ^1\text{P})$ and N_2O , Bourguignon et al. [10] concluded that $\text{Mg}(^1\text{P})$ is much more reactive than $\text{Mg}(^3\text{P})$. They further showed that, due to radiation trapping, the apparent lifetime of $\text{Mg}(^1\text{P})$ ($T_1 > 20\ \mu\text{s}$) can be many orders of magnitude larger than the natural lifetime ($\tau = 1.9\ \text{ns}$) measured by Breckenridge and Umamoto [9]. Thus, MgO is efficiently formed by the reaction,



Reaction (3) can be monitored by observing the green band system associated with the decay of the transient $B\ ^1\Sigma^+$ state ($\tau = 32.7\ \text{ns}$) [11],



In a Broida-type oven, $\text{Mg}(^3\text{P})$ is apparently formed from $\text{Mg}(^1\text{S})$ by electrons emitted by the heating filament [14], and can then produce $\text{Mg}(^1\text{P})$ by triplet-triplet annihilation [10],



The observation of chemiluminescence from the reaction of magnesium with $\text{N}_2\text{O}/\text{He}$ [15] and $\text{N}_2\text{O}/\text{CO}/\text{He}$ [16] mixtures, at pressures of several mbars, is most probably due to such a mechanism [10].

Improvement of the reactivity of magnesium by exciting the atoms with an excimer laser [17] or an electrical discharge [18] has been reported earlier. In the present study on the infrared spectrum of $\text{MgO}(X\ ^1\Sigma^+)$, the latter method was used to produce magnesium oxide monomers at pressures as low as a few Pa.

2. Experimental

The diode-laser flame spectrometer used to study the infrared spectrum of monomeric magnesium oxide has been described earlier [19]. Two diode lasers were used in the present study. Calibration was made with respect to C_2H_2 #1, C_2H_4 #1 and CO_2 [20], by simultaneously measuring sample, reference and etalon absorption maxima. From the variance of several independent measurements, the precision in the wavelengths of the weak MgO transitions was estimated to be $0.001\ \text{cm}^{-1}$.

Initially, we tried to produce MgO by reacting hot magnesium vapor with N_2O . Under conditions similar to those used for CaO [13], SrO [21] and BaO [19] (a partial N_2O pressure of 2 Pa and a metal evaporation rate of about $10\ \text{g h}^{-1}$) only a tiny flame was observed just above the oven. Although plenty of magnesium evaporated, hardly any oxide was formed and black metal deposits were observed on the walls of the reactor. We therefore decided to stimulate the MgO formation by means of a dc discharge in the reaction vessel.

Several arrangements of electrodes were tried but found to be inadequate for maintaining a stable discharge. For instance, with the oven as electrode the metal evaporation rate became uncontrollable whereas unprotected electrodes always sparked as soon as oxide deposited on them. But in all the preliminary experiments, intensive green emissions from the plasma and deposits of solid magnesium oxide indicated that the magnesium vapor indeed reacted with N_2O .

The final setup used for the spectroscopy of MgO is shown in fig. 1. Two water-cooled stainless-steel electrodes (15 cm long, 6 mm outer-diameter tubing) were situated in side arms attached to the reaction vessel. To prevent deposition of MgO on their surfaces, additional N_2O gas inlets were situated close to the electrodes. The distance between the electrodes was 70 cm. A high-voltage generator with, in series, a $390\ \Omega$ ballast resistor and a high-voltage modulator [22] enabled on-off modulation of the discharge from dc to 50 kHz. With this arrangement,

#1 Measured with the Bruker IFS 120 HR FTIR spectrometer and calibrated against CO_2 [20].

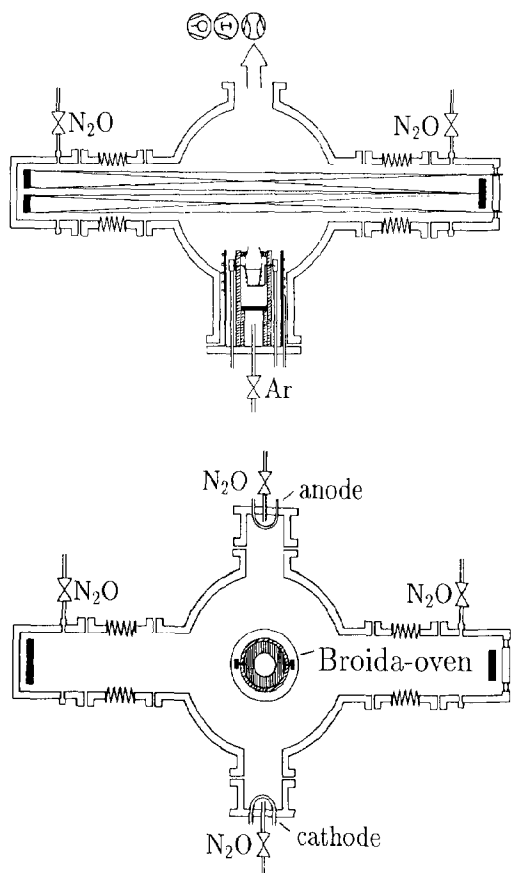


Fig. 1. Scale drawing of the reaction vessel with 1 m White-cell, Broida-type oven, and electrodes. Upper part: side view, lower part: top view. The symbols in the upper part indicate the differential pumping system used: a large oil-booster pump (Leybold PV NW 250/350, used at low pressures only) and a Roots blower (Leybold WSU 500) with an appropriate roughing pump (Leybold VP 200) in series.

a stable discharge in the medium containing N_2O , Ar and Mg vapor was obtained.

The discharge was started with a total pressure of 3 Pa (2 Pa N_2O introduced from the mirrors of the multireflection cell and the electrodes and 1 Pa Ar from the oven). The potential measured at the electrodes was 1.5 kV, the current 50 mA. Next, the oven was heated to about 900 K. As soon as magnesium evaporated, the color of the emission in the bulb changed from weak purple (typical for N_2O /Ar discharges) to green (probably due to the green band of MgO [1–3]) and became even more intense upon an increase of the N_2O partial pressure to about 5 Pa.

Under these conditions, a few lines were detected (e.g. at 740.704 and 747.752 cm^{-1}) which were only present as long as magnesium evaporated from the oven. However, no lines with the expected wave-number spacing for $X^1\Sigma^+$ MgO rovibrational transitions could be detected.

In the following sessions, the N_2O partial pressure was gradually increased to about 30 Pa. At this pressure, a white diffuse flame was observed in the center of the bulb whereas the green emission was only present in the regions close to the oven and the electrodes. In this type of flame, lines with appropriate spacing for the $\nu=1\leftarrow 0$ band of $X^1\Sigma^+$ MgO were detected. After the flame conditions were optimized on the signals, it appeared that the line intensities peaked when the infrared laser beam crossed the region where the flame changed from green to white. All rovibrational transitions of the $\nu=1\leftarrow 0$ and $\nu=2\leftarrow 1$ bands of MgO were measured with similar conditions. For signal enhancement, conventional source modulation of the laser ($f=5$ kHz) and 2f phase-sensitive detection were used. With 28 transversals of the diode-laser radiation through the White cell, the effective optical path in the flame was 8–9 m.

Optical fringing was a serious problem in the present study. Even for a well-aligned system where lines with $10^{-3}\%$ absorbance could be detected, the situation changed drastically as soon as magnesium evaporated. Probably due to scattering of diode-laser radiation at larger MgO particles, the fringes increased by several orders of magnitude. They could be partly suppressed by readjustment of the laser and by optimizing of the modulation depth during the short period (less than 1 h) available for data acquisition.

Experiments aimed at detecting the $X^1\Sigma^+$ MgO transitions by concentration modulation using a 20 Hz–20 kHz on–off modulation failed. It appeared that at the pressure (30 Pa) needed to produce MgO, the signals decreased only slowly ($\tau \approx 300$ s) after the discharge was switched off. With N_2O pressures higher than 650 Pa, it was even possible to cultivate a moderate flame without discharge, but no lines could be observed under such high-pressure conditions.

3. Results

The strongest rovibrational transitions ($\Delta I/I \approx 10^{-4}$) of the $\nu=1 \leftarrow 0$ band of ^{24}MgO (79% in natural abundance) could be measured with a S/N ratio of about 10. Lines due to ^{25}MgO (10%) and ^{26}MgO (11%) were not observed. The 22 transitions detected for ^{24}MgO , 15 of the fundamental band and 7 of the first hot band, are listed in table 1. Fig. 2 shows a part of the spectrum between 778.1 and 778.2 cm^{-1} .

Molecular constants for the $X^1\Sigma^+$ state of ^{24}MgO were derived using the equation,

$$T_{v,J} = G_v + B_v J(J+1) - D_v J^2(J+1)^2. \quad (6)$$

The accuracy in the positions of the infrared lines was estimated as 0.001 cm^{-1} . Rotational transitions for $\nu=0, 1$ and 2 and their uncertainties, taken from the literature [8], were also included in the simultaneous least-squares fit of the data of both bands. The constants are not given here, since they are essentially the same as the $X^1\Sigma^+$ state constants re-

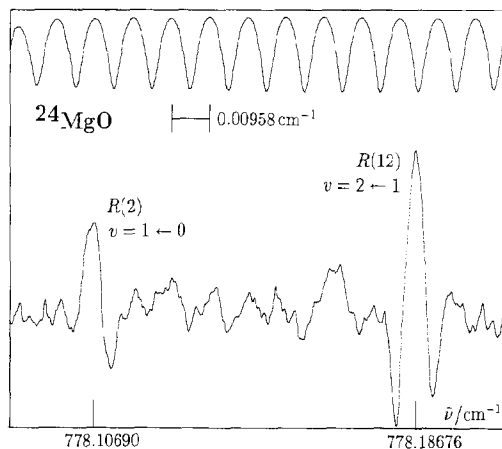


Fig. 2. Diode-laser spectrum of two MgO transitions and simultaneously recorded etalon fringes.

sulting from the final fitting described below.

Azuma et al. [7] have obtained Doppler-limited laser-induced fluorescence spectra of the $B^1\Sigma^+ - X^1\Sigma^+$ ($\nu=0 \leftarrow 0$ and $\nu=1 \leftarrow 1$) electronic band of ^{24}MgO . From these data alone, the vibrational spac-

Table 1
Observed line positions of ^{24}MgO

J'	J''	ν'	ν''	Observed (cm^{-1})	Obs. - calc. ^{a)} (10^{-5} cm^{-1})	Uncertainty (10^{-5} cm^{-1})
6	7	1	0	766.50761	-48	100
12	13	1	0	759.04598	95	100
15	16	1	0	755.17478	44	100
18	19	1	0	751.21150	-43	100
26	27	1	0	740.20288	-7	100
27	28	1	0	738.78135	-74	100
31	32	1	0	733.00128	84	100
3	2	1	0	778.10690	-11	100
10	9	1	0	785.58731	-107	100
15	14	1	0	790.60444	42	100
16	15	1	0	791.57369	-25	100
17	16	1	0	792.53305	34	100
20	19	1	0	795.34193	4	100
27	26	1	0	801.50152	52	100
32	31	1	0	805.55626	-38	100
7	8	2	1	755.07141	4	100
18	19	2	1	741.10737	-83	100
20	21	2	1	738.43655	-9	100
13	12	2	1	778.18676	-49	100
17	16	2	1	782.04527	-15	100
24	23	2	1	788.36541	62	100
28	27	2	1	791.72608	89	100

^{a)} From the final least-squares refinement on microwave, optical, and infrared data (see table 2).

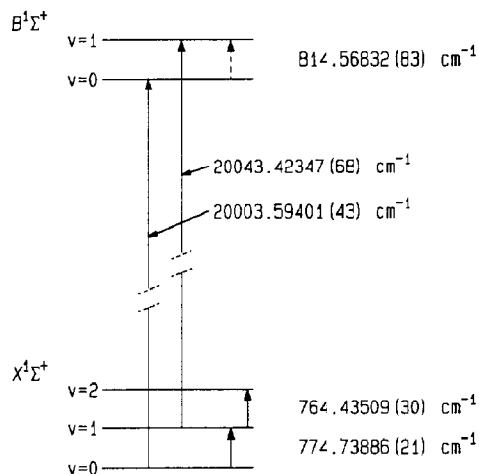


Fig. 3. Energy levels of the X $^1\Sigma^+$ and the B $^1\Sigma^+$ states of MgO.

ing of the short-lived B $^1\Sigma^+$ state is not determined (see fig. 3). However, the additional data from the present study of $v=1 \leftarrow 0$ of the X $^1\Sigma^+$ state give sufficient information to obtain $G_1 - G_0$ of B $^1\Sigma^+$ MgO with high precision. In the last column of table 2, a

set of molecular constants is listed obtained from a merged least-squares fit on 137 optical [7], 8 microwave [8] and 22 infrared line positions of ^{24}MgO .

4. Discussion

Since the study of Lagerqvist and Uhler [2], more than four decades ago, the accuracy of the molecular constants has increased by several orders of magnitude. If one assumes an error of 10 in the last digit they quoted, their earlier results were, however, completely correct.

Information from optical, infrared and microwave spectroscopy contributes to each of the molecular constants in the last column of table 2. But intermediate least-squares calculations show that the small error limits on the B and D constants of the X $^1\Sigma^+$ state are mainly due to the accuracy of the rotational line positions from the microwave data (third column of table 2) [8]. The infrared data from the present study determine the vibrational band centers. They can be determined from the infrared data

Table 2
Spectroscopic constants of ^{24}MgO (in cm^{-1})

^{24}MgO		From optical data		From mw data [8]	From optical [7], mw [8] and IR data (this work)
		ref. [2]	ref. [7]		
X $^1\Sigma^+$	B_0	0.5718	0.57204(5) ^{a)}	0.57204165(11) ^{b)}	0.57204169(6) ^{c)}
	B_1	0.5668	0.56671(8)	0.56671121(26)	0.56671121(7)
	B_2	0.5618		0.56137422(49)	0.56137456(15)
	$10^6 D_0$	1.23	1.23(2)	1.2343(8)	1.2350(6)
	$10^6 D_1$	1.25	1.17(14)	1.2373(11)	1.2368(7)
	$10^6 D_2$	1.27		1.2404(16)	1.2425(11)
	$G_1 - G_0$	774.70			774.73886(21)
	$G_2 - G_1$	764.34			764.43509(30)
B $^1\Sigma^+$	B_0	0.5799	0.58009(5)		0.5800950(22)
	B_1	0.5754	0.57525(8)		0.5752451(20)
	$10^6 D_0$	1.16	1.15(2)		1.1623(18)
	$10^6 D_1$	1.17	1.10(14)		1.1653(11)
	$G_1 - G_0$	814.56			814.56832(83)
B $^1\Sigma^+$ - X $^1\Sigma^+$	T_{00}	20003.57	20003.594(2)		20003.59401(43)
	T_{11}	20043.43	20043.422(2)		20043.42347(68)

^{a)} The uncertainties represent a 95% confidence limit.

^{b)} Errors quoted in parentheses are one standard deviation. The constants are calculated from the Y_j constants given by Törning and Hoeft [8].

^{c)} Errors quoted in parentheses are one standard deviation.

alone, but the standard deviations of G_1-G_0 and G_2-G_1 decreased by one order of magnitude after inclusion of the microwave data in the fit. A similar conclusion can be drawn by comparing the results for the B $^1\Sigma^+$ constants in the second and fourth column of table 2. For both refinements, the same set of optical line positions for the 0-0 and 1-1 bands of the B $^1\Sigma^+$ -X $^1\Sigma^+$ system was employed. Inclusion of the infrared and microwave data of the X $^1\Sigma^+$ state not only gives access to G_1-G_0 , but also increases the precision of the B and D constants of the B $^1\Sigma^+$ state by an order of magnitude. The latter result is due to the removal of the strong correlation between X $^1\Sigma^+$ and B $^1\Sigma^+$ constants by including accurate ground-state data.

Acknowledgement

We are grateful to Klaus Lattner for the recording of the reference spectra and Brenda P. Winnewisser for a critical reading of the manuscript. One of us (SC) thanks the Alexander-von-Humboldt foundation for a fellowship. This work is financially supported by the Deutsche Forschungsgemeinschaft.

References

- [1] A. Lagerqvist, Arkiv Nat. Astr. Fysik 29 A (1943) 4.
- [2] A. Lagerqvist and U. Uhler, Arkiv Fysik 1 (1949) 459.
- [3] P.C. Mahanti, Phys. Rev. 42 (1932) 609.
- [4] T. Ikeda, N. Bew Wong, D.O. Harris and R.W. Field, J. Mol. Spectry. 68 (1977) 452.
- [5] P.J. Evans and J.C. Mackie, Chem. Phys. 5 (1974) 277.
- [6] P.C.F. Ip, Ph.D. thesis, Department of Chemistry, Massachusetts Institute of Technology, USA (1983).
- [7] Y. Azuma, T.R. Dyke, G.K. Gerke and T.C. Steimle, J. Mol. Spectry. 108 (1984) 137.
- [8] T. Törring and J. Hoefl, Chem. Phys. Letters 126 (1986) 477.
- [9] W.H. Breckcnridge and H. Umemoto, J. Chem. Phys. 77 (1982) 4464.
- [10] B. Bourguignon, J. Rostas and G. Taieb, J. Chem. Phys. 77 (1982) 2979.
- [11] P.J. Dagdigian, J. Chem. Phys. 76 (1982) 5375.
- [12] D.R. Yarkony, J. Chem. Phys. 78 (1983) 6763.
- [13] H.G. Hedderich and C.E. Blom, J. Chem. Phys. 90 (1989) 4660.
- [14] D.C. Hartman and J.S. Winn, J. Chem. Phys. 74 (1981) 4320.
- [15] D.J. Bernard, W.D. Slafer and J. Hecht, J. Chem. Phys. 66 (1976) 1012.
- [16] D.J. Bernard and W.D. Slafer, J. Chem. Phys. 66 (1976) 1017.
- [17] B. Bourguignon, Ph.D. thesis, Université de Paris-Sud, France (1986).
- [18] J. Schamps and G. Gandara, J. Chem. Phys. 77 (1982) 2979.
- [19] H.G. Hedderich and C.E. Blom, J. Mol. Spectry. 140 (1990) 103.
- [20] G. Guelachvili and K. Narahari Rao, Handbook of infrared standards (Academic Press, New York, 1986).
- [21] H.G. Hedderich, C.E. Blom and A.G. Maki, in preparation.
- [22] C.E. Blom, K. Möller and R.R. Filgueira, Chem. Phys. Letters 140 (1987) 489.